HHS Public Access

Author manuscript

Cancer Gene Ther. Author manuscript; available in PMC 2023 June 01.

Published in final edited form as:

Cancer Gene Ther. 2022 December ; 29(12): 1840–1846. doi:10.1038/s41417-022-00452-7.

HDAC11 activity contributes to MEK inhibitor escape in uveal melanoma

Sathya Neelature Sriramareddy[1], **Fernanda Faião-Flores**[1], **Michael F. Emmons**[1], **Biswarup Saha**[1], **Srikumar Chellappan**[1], **Clayton Wyatt**[2], **Inna Smalley**[2], **Jonathan D. Licht**[3], **Michael A. Durante**[4], **J. William Harbour**[4], **Keiran S.M. Smalley**[1,*]

[1]The Department of Tumor Biology, The Moffitt Cancer Center & Research Institute, 12902 Magnolia Drive, Tampa, FL, USA.

[2]Department of Cancer Physiology, The Moffitt Cancer Center & Research Institute, 12902 Magnolia Drive, Tampa, FL, USA.

[3]University of Florida Health Sciences Center, Gainesville, FL,

[4]Sylvester Cancer Center, University of Miami, Miami, FL.

Abstract

We previously demonstrated that pan-HDAC inhibitors could limit escape from MEK inhibitor (MEKi) therapy in uveal melanoma (UM) through suppression of AKT and YAP/TAZ signaling. Here, we focused on the role of specific HDACs in therapy adaptation. Class 2 UM displayed higher expression of HDACs 1, 2 and 3 than Class 1, whereas HDACs 6, 8 and 11 were uniformly expressed. Treatment of UM cells with MEKi led to modulation of multiple HDACs, with the strongest increases observed in HDAC11. RNA-seq analysis showed MEKi to decrease expression of multiple HDAC11 target genes. Silencing of HDAC11 significantly reduced protein deacetylation, enhanced the apoptotic response to MEKi and reduced growth in long-term colony formation assays across multiple UM cell lines. Knockdown of HDAC11 led to decreased expression of TAZ in some UM cell lines, accompanied by decreased YAP/TAZ transcriptional activity and reduced expression of multiple YAP/TAZ target genes. Further studies showed this decrease in TAZ expression to be associated with increased LKB1 activation and modulation of glycolysis. In an *in vivo* model of uveal melanoma, silencing of HDAC11 limited the escape to MEKi therapy, an effect associated with reduced levels of Ki67 staining and increased cleaved caspase-3. We have demonstrated a novel role for adaptive HDAC11 activity in UM cells, that in some cases modulates YAP/TAZ signaling leading to MEKi escape.

*To whom correspondence should be addressed, Tel: 813-745-8725, Fax: 813-449-8260, keiran.smalley@moffitt.org.

Author contributions: SNS, FF-F, MFE, BS, CW performed the experiments. SNS, MFE, SC, JDL, IS, MAD, JWH and KSMS analyzed the data. SNS, MFE, IS and KSMS wrote the manuscript. MAD, JWH, JDL and KSMS edited the manuscript. All authors read and approved the final manuscript.

Conflict of interest: The authors declare no conflict of interest

Introduction

Uveal melanoma is the most common primary cancer of the eye, derived from melanocytes residing in the uveal tract of the eye. Disseminated disease is infrequent at diagnosis, but about half of patients eventually succumb to metastases (1), most frequently to the liver. There are no effective treatments for metastatic UM, including immune checkpoint inhibitors, which are now standard for metastatic cutaneous melanoma (2). Patients are stratified into groups with low (Class 1) vs. high (Class 2) risk of metastasis based on a validated 15-gene expression signature developed by our group (3). Class 1 tumors show greater differentiation and are divided into Class 1a and 1b with a 5-year metastasis risk of 2%, and 21% (4). Class 2 tumors lose melanocyte differentiation, express primitive neuroectoderm genes, and have a 5-year metastatic risk of 70–80% (4).

More than 90% of uveal melanomas harbor activating mutations in the small G-proteins GNAQ or GNA11 (the former more common) which activate the mitogen activated protein kinase (MAPK) pathway (5, 6). Constitutive signaling in cascades including the PI3K/AKT/mTOR, WNT/β-catenin and the YAP pathways are also frequently seen in UM (7–12). Once established in the liver, UM responds poorly to targeted therapy, immunotherapy and chemotherapy. Current efforts are focused on targeted therapies against the kinases downstream of GNAQ/GNA11 such as the MEKi selumetinib (AZD6244) which improved progression-free survival in UM compared to either dacarbazine or temozolomide (13). However, a subsequent phase III trial of selumetinib plus dacarbazine showed no improvement compared to dacarbazine alone (14). Previous work from our lab using phospho-proteomics and RNA-seq to map the patterns of adaptation of UM cells to MEKi treatment (15) identified increased YAP and AKT signaling as important escape mechanisms (15). Drug screening showed that pan-histone deacetylase (HDAC) inhibition limits adaptive signaling and improves response (16).

It is not yet clear which HDACs are important for MEK inhibitor escape in uveal melanoma. Studies from cutaneous melanoma have elucidated a role for HDAC8 in the escape of BRAF mutant melanoma cells from BRAF inhibitor therapy (17). In uveal melanoma, pan-HDAC inhibitors shifted the expression profile of Class 2 UM to that of Class 1 (18). Work from our group further supports a role for HDAC4 and HDAC1 in maintaining the phenotype conferred by BAP1 loss. We here provide new data that MEK inhibition leads to increased HDAC11expression in uveal melanoma cells and that silencing of HDAC11 can sensitize some UM cells to MEKi, in part through deregulation of adaptive YAP/TAZ signaling.

Materials and methods

Reagents

RPMI culture medium was purchased from Corning (Corning, NY). Fetal bovine serum (FBS) was purchased from Sigma Chemical Co. (St. Louis, MO). Trypsin, pen/strep antibiotics, and puromycin were purchased from Gibco (Grand Island, NY). Trametinib (MEK inhibitor) was purchased from Selleckchem (Houston, TX). Antibodies for Western Blot: Anti-HDAC1 (#2062, from Cell Signaling Technology (Danvers, MA), anti-HDAC2 (#2540 CST), The anti-HDAC3 and anti-HDAC8 antibodies were described in refs. 17,

HDAC11(#58442, CST). Anti-HDAC6 (#H-300, sc-11420) was purchased from Santa Cruz Biotechnologies. Cleaved PARP (Asp214) (#D64E10) (#5625 CST), phospho LKB1 (#3482, CST), total LKB1 (#3050, CST). Anti-YAP1 antibody (#H00010413-M01, Abnova). Anti-Vinculin (#G8796) and anti-GAPDH (#V9131) were purchased from Millipore Sigma (Bedford, MA).

Uveal melanoma cell lines

The uveal melanoma cell lines 92.1, Mel270, Mel290 and MP41 were obtained from Dr. J William Harbour (University of Miami), OCM1, OCM3, OCM8 and OMM1 were from Dr. David Morse (Moffitt Cancer Center) used as previously described (19). All uveal melanoma cell lines were cultured in RPMI-1640 supplemented with 10% FBS, L-glutamine and antibiotics at 5% CO_2. All cells were tested for mycoplasma contamination every month using the Plasmo test-Mycoplasma Detection Test (Invivogen, San Diego, CA). Each cell line was authenticated using the Human STR human cell line authentication service (ATCC) and frozen stocks of cells were discarded after 10 passages.

HDAC expression analysis from scRNA-seq data

The Seurat object containing Single-cell RNA-seq data from 11 uveal melanoma samples from previously published work from our group was obtained (20). The data was analyzed using R (4.1.0) and the Seurat (4.0.4) package (21). The Seurat object was updated to Seurat v3 format using the UpdateSeuratObject() function. The FindNeighbors() and RunUMAP() functions with dims set to 1:20 were used to calculate UMAP representation. The DimPlot() and VlnPlot() functions were used to generate plots from the 59,915 cells.

Identification of HDAC11 target genes from RNA-Seq

RNA-Seq data for MEKi treated uveal melanoma cell lines were acquired from a previously published study (15). HDAC11 transcriptional targets were identified and analyzed using Enrichr software (22). Pathway analysis was performed using the ShinyGO v0.741: Gene Ontology Enrichment Analysis platform (http://bioinformatics.sdstate.edu/go/). Hallmark pathways were analyzed using the MSigDB database. Transcription factor target enrichment was determined using the ChEA.2016 data- base.

Colony formation assay

1×10^3 cells were plated and allowed to attach overnight. The medium and drug/vehicle was replaced every two days for 4 weeks. After the specific treatments for each experiment, colonies were stained with crystal violet dye, as previously described (23). Experiments were performed three times in triplicate.

Flow cytometry for apoptosis analysis

1×10^5 cells were plated and allowed to attach overnight. After the specific treatments for each experiment, Annexin V staining quantification was performed using FlowJo software as previously described (24). All experiments were performed three times in duplicate.

Immunoblotting

Cells were plated and allowed to attach overnight. After the specific treatments for each experiment, proteins were extracted and blotted as previously described (25). Total and phospho-proteins were analyzed and then the membranes were stripped and reprobed for GAPDH/vinculin/β-actin. Data shown are one representative experiment from three independent experiments.

HDAC activity assays

Histone deacetylase (HDAC) activity was measured using the Epigenase HDAC Activity/ Inhibition Direct Assay Kit (Epigentek; P-4034). The kit provided one microplate containing the respective substrate coated onto the wells. Nuclear extract samples (7.5μg) were mixed with the assay buffer and the assay was performed according to manufacturer's instructions. Data shown is mean results from three independent experiments.

Quantitative real-time PCR

Total RNA was isolated using Qiagen's Rneasy Mini Kit (Qiagen, Hilden, Germany). 1 μg of RNA was converted into cDNA using iScript cDNA synthesis kit (Bio-Rad). Levels of mRNA were analyzed using quantitative reverse transcription-PCR (qRT-PCR) that was performed using Bio-Rad CFX96 Real time system. Data was normalized using GAPDH as an internal control and fold change was calculated by $2^{-\Delta\Delta Ct}$ method. Data shown are from three independent experiments with two replicates per condition.

Transfection and luciferase assay

A YAP/TAZ-responsive synthetic promoter driving reporter plasmid, 8xGTIIC-luciferase (Addgene, #34615) and control plasmid, pRL Renilla luciferase from Promega (#E2231) were used in this assay. 92.1, Mel270 and MP41 cells (120×10^3 cells per well in 6-well plates) were transfected with the constructs using FuGENE (Promega; #31985–070) for 8h. Media was changed for another 12h prior to the MEKi (10nM and 30nM) treatments for another 48h. Harvested cells were washed once with PBS and luciferase assay was performed according to the manufacturer protocol using Dual-Luciferase® Reporter Assay System (Promega, #E1910)) and plotted the values normalized against Control without any inhibitor treatment. Data shown are from three independent experiments performed in duplicate.

Seahorse metabolic analysis

8.0×10^5 cells were plated per well and allowed to attach overnight in the Seahorse 96-well cell culture plate. Glycolysis was measured on the Seahorse XFe96 instrument using the Glycolysis Stress Test Kit (Agilent, Santa Clara, CA) according to manufacturer protocol. Data shown in Figure 3E and 3F is one representative experiment out of two independent experiments, visualizing 12 technical replicates within the experiment. Error bars represent Standard Error of the Mean. Student's t-test was performed on each of the 3 readings after oligomycin injection, representing the glycolytic reserve of each cell line. **** = $P<0.0001$.

In vivo mouse model:

Eight-week-old female CBySmn. CB17-Prdkc scid/j mice (Stock No: 001803 – Jax Labs) were subcutaneously injected with 1.0×10^6 MP41 shCTRL or shHDAC11 uveal melanoma cells into each flank. The tumors were allowed to grow for 3 weeks and mice were randomly separated with similar average initial tumor volumes, with a total of 5 mice per group. Sample size was estimated from previous studies of MEKi therapy in this mouse uveal melanoma model (15). The mice were treated with MEKi (trametinib, 1 mg/kg gavage, daily) for 32 days. The control group received vehicles (0.5% methylcellulose + 0.5% Tween-80 molecular grade sterile water). Mouse weight and tumor volumes (1/2 " L " W2) were measured every 48 hours. All animal experiments were carried out in agreement with ethical regulations and protocols approved by the University of South Florida Institutional Animal Care and by The Institutional Animal Care and Use Committee (IACUC number IS00007140R). The IACUC protocol did not permit survival to be an experimental endpoint. The investigators involved were not blinded to the treatment groups.

Immunohistochemical staining

Excised tumor samples were fixed in buffered formalin and embedded in paraffin and sectioned at 5 μm were stained for Ki67 (Abcam, ab16667, Waltham, MA) and cleaved caspase 3 (#9661, Cell Signaling, Danvers, MA). Slides were viewed and acquired using the Aperio ScanScope (Leica Biosystems Inc, Buffalo Grove, IL). To quantify staining, 5 fields of view were randomly selected for each tumor from treatment group. Ki67 and cleaved caspase 3 expression were determined by the positive nuclei and cytosolic within a given compartments respectively.

Statistical analysis

Results are expressed as mean ± standard deviation of at least three independent experiments. One-way analysis of variance (ANOVA) was used followed by a TUKEY-KRAMER posttest to test for multiple comparisons with a given significance level of $p<0.05$. Significant differences between the control and treated groups are indicated by *=$p<0.05$, **=$p<0.01$, ***=$p<0.005$, and #=$p>0.05$.

Results

Uveal melanoma cell lines express multiple HDACs, some of which are upregulated in response to MEKi

Although our previous work suggested that pan-HDAC inhibition could limit escape from MEKi therapy, little is known about which specific HDAC (s) are involved in this response. To address this we began by profiling a panel of uveal melanoma cell lines and human clinical samples for HDAC expression. The majority of uveal melanoma cell lines profiled expressed detectable and similar levels of HDAC1, 2, 3 6, 8 and 11 (Figure 1A). Analysis of a previously published clinical uveal melanoma single cell dataset (20) identified higher expression of HDAC1, 2 and 3 in Class 2 vs. Class 1 uveal melanoma (Figure 1B) and showed uniform expression of HDAC6 and 11 across Class 1 and Class 2 uveal melanoma.

Previous studies in cutaneous melanoma showed that inhibition of MAPK signaling led to increased expression and activity of HDAC8 (17). We found that treatment of the 92.1 UM cell line with trametinib led to increased expression of multiple HDACs including, HDAC 1, 2, 6, 8 and 11 (Figure 1C). Among these HDAC11 showed the greatest increase upon MEK inhibition in 92.1 cells. Repeat of these studies across the MP41, OCM1 and Mel270 UM cell lines demonstrated that although MEKi treatment led to diverse effects on HDAC expression, only HDAC2 and HDAC11 showed a consistent increase in all of the cell lines evaluated (Figure 1C). A previously published RNA-seq analysis (15) of genes decreased in UM cells following treatment with the MEKi inhibitor trametinib identified multiple genes known to modulated by HDAC11 including CDT1, E2F4, E2F5, EGR1, MYC and PN1 (Figure 1D). A pathway analysis of RNA-Seq data confirmed these findings with MYC target genes being the most significantly enriched pathway upon treatment with trametinib in 92.1, MP41, and Mel270 cell lines (Supplemental Figure 1A-1C). An additional analysis was performed looking at transcription factor targets enriched upon trametinib treatment with the HDAC11 targets E2F4, EGR1 and MYC targets being significantly altered in UM cell lines (Supplemental Figure 1D-1F).

Silencing HDAC11 sensitizes UM cell lines to MEKi

As HDAC11 showed the greatest increase in expression upon trametinib treatment we next asked if this specific HDAC was responsible for histone deacetylation. We began by generating 92.1 and Mel270 UM cells that had HDAC11 stably knocked down by shRNA (Figure 2A). It was noted that silencing of HDAC11 led to a statistically significant reduction in total HDAC activity (Supplemental Figure 2) and deacetylation (Figure 2B). We next turned our attention to whether upregulated HDAC11 expression played any role in the escape from MEKi therapy. Having confirmed that silencing of HDAC11 expression was effective following trametinib treatment (Figure 2A), we next demonstrated that this was associated with an increased apoptotic response in Mel270, MP41 and 92.1 cells (Figure 2C). This increased MEKi-induced apoptotic response seen following HDAC11 knockdown was accompanied by an increased cleavage of PARP (Figure 2D). Over long-term MEKi treatment, HDAC11 silencing limiting escape from therapy as measured by a decrease in drug resistant colonies formation by MP41 and 92.1 UM cells (Figure 2E).

In some UM cell lines, silencing of HDAC11 deregulates YAP/TAZ signaling

Our previous work identified escape from MEKi therapy to be associated with increased AKT signaling and an upregulation of YAP/TAZ signaling (15). Initial studies showed knockdown of HDAC11 to have little effect upon adaptive AKT signaling (not shown). Instead, we found that HDAC11 silencing impacted expression of TAZ in Mel270 cells, but not in 92.1 (Figure 3A). The effects of HDAC11 upon YAP/TAZ signaling was also supported by YAP/TAZ reporter assays, which showed HDAC11 silencing to reduce basal YAP levels, and then partly suppress the MEKi-induced increases in YAP1 activity (Figure 3B). qRT-PCR analyses also demonstrated that HDAC11 silencing suppressed levels of YAP-target genes (Figure 3C).

YAP/TAZ signaling can be regulated by liver kinase B1 (LKB1)/ 5’ adenosine monophosphate protein kinase (AMPK) which are known targets of HDAC11 (26). UM

cell lines such as Mel270 which had reduced TAZ expression in response to HDAC11 silencing also showed increased expression of phospho-LKB1 (Figure 3D). The Seahorse Glycolysis stress test showed that knockdown of HDAC11 in Mel270 UM cells resulted in a decrease of glycolytic capacity of the cells, with a complete loss of glycolytic reserve compared to control cells (Figure 3E). Meanwhile, knockdown of HDAC11 did not result in any significant shift in glycolysis or glycolytic capacity of MP41 cells (Figure 3F).

Silencing of HDAC11 is associated with enhanced responses to the MEKi trametinib in *in vivo* models of uveal melanoma.

Finally, we asked whether HDAC11 was required for the escape of uveal melanoma cells from MEKi therapy *in vivo*. Isogenic HDAC11 expressing and silenced MP41 cells were grown as flank tumors in immunocompromised mice and then treated with the MEKi trametinib (1mg/kg) for up to 32 days. Analysis of tumor growth over time demonstrated that HDAC11 was required for the efficient growth of MP41 tumors (Figure 4A). It was further noted that silencing of HDAC11 enhanced the anti-tumor effects of trametinib, with little tumor growth being observed under therapy (Figure 4A). Immunohistochemical analysis of the tumors at endpoint demonstrated that although the MEKi alone significantly reduced levels of cell proliferation (Ki67) and increased cell death (Caspase-3 cleavage) (Fig 4B and 4C), these effects were more pronounced when HDAC11 was silenced. It thus appeared that silencing of HDAC11 enhanced the therapeutic effects of MEKi therapy *in vivo* models of uveal melanoma.

Discussion

Many cancers are dependent upon signaling through the mitogen-activated protein kinase (MAPK) pathway for their growth and survival. This is typified by cutaneous melanoma which has a high frequency of *BRAF* and *NRAS* mutations and seems to be uniquely "addicted" to MEK/ERK signaling (27). Uveal melanoma is instead characterized by mutations in the small G-proteins GNAQ and GNA11, which also drive signaling through MAPK, as well as other pathways including PKC (6). In patients with metastatic uveal melanoma, responses to MEK inhibitors are usually short-lived (28). In previous work, we used multi-omics approaches to demonstrate that MEK inhibition led to a rapid increase in signaling through AKT, G-protein coupled receptors (GPCRs) and YAP that was associated with therapeutic escape (15). This adaptive signaling could be overcome through use of pan-HDAC inhibitors, and there was evidence that the combination of a MEK and a pan-HDAC inhibitor (Panobinostat) could overcome therapy escape - leading to prolonged responses in mouse models of uveal melanoma liver metastasis (15).

Melanoma cells express multiple HDACs, and it is likely that each subserves different functions. In *BRAF*-mutant cutaneous melanoma, BRAF inhibition (and other stresses) upregulates expression and function of HDAC8, which can drive therapy escape through increased EGFR-mediated MAPK signaling (17). There is also evidence that HDAC3 inhibition can suppress DNA-repair pathways in melanoma cells, increasing the effectiveness of MAPK-targeted pathway inhibitors (29).

Immunohistochemical studies of primary uveal melanoma have identified the expression of multiple HDACs including HDAC1, 2, 3, 4, 6 and sirtuin 2 (30). Another analysis of 64 uveal melanomas reported expression of HDACs 1, 3, 4 and 8 in high-risk UM. In the current study, we identified HDAC11 as being upregulated following MEK inhibitor treatment. Silencing of HDAC11 reduced global deacetylation in melanoma cells and sensitized uveal melanoma cells to MEKi-induced cell death. HDAC11 is the smallest known HDAC (39 kDa) and is the sole type IV HDAC (31). This enzyme is highly conserved in organisms as diverse as plants and invertebrates (32). HDAC11 is expressed in multiple organs including the heart, smooth muscle, kidneys and cells of the central nervous system/neural crest and has multiple effects upon immune regulation and has been implicated in the induction of CD4+ T-cell tolerance through the regulation of multiple cytokines, including IL-10 (33). There is evidence that HDAC11 plays a role in cell survival and suppression of apoptosis with studies in neuroblastoma demonstrating that HDAC11 silencing increases apoptosis (34). In liver cancer, HDAC11 is known to negatively regulate cell death by suppressing p53 expression (35).

There is emerging evidence that HDAC11 also regulates metabolism with recent studies demonstrating that HDAC11-knockout mice are resistant to obesity (36). In cancer cells, HDAC11 inhibits LKB1 expression, with studies showing that HDAC11 silencing leads to increased AMPK expression and a decrease in glycolysis (26). Our studies supported this and demonstrated that in some UM cell lines (such as Mel270) HDAC11 silencing increased LKB1 signaling and reduced rates of glycolysis. In addition to its effects upon metabolism, the LKB1/AMPK axis can also directly suppress YAP/TAZ activity through increased phosphorylation (37, 38). An additional layer of regulation occurs following the phosphorylation of angiomotin-like 1 (ATMOL1) by AMPK leading to activation of the LATS1/2 Hippo pathway kinases and the inhibition of YAP/TAZ (39). Recent work demonstrated that AMPK is upregulated in Class 2, *BAP1* mutant melanoma, perhaps suggesting that metabolic reprogramming is required for UM metastasis (40).

It is worth noting that HDAC11 did not regulate AMPK/LKB1 in all UM cell lines, or even impact YAP/TAZ signaling, despite increasing sensitivity to MEKi treatment. Further studies will be required to fully address the mechanisms by which HDAC11 upregulation contributes to MEKi escape across the UM landscape. It is also of interest to determine whether HDAC11-regulated transcriptional networks are specific to stresses associated with MEKi or represent a more conserved stress adaptation program in UM. In summary, we have outlined a potential role for HDAC11 in the therapeutic adaptation of UM to MEKi. It is likely that use of HDAC11 inhibitors could be one potential strategy to improved therapeutic responses to MEKi in metastatic UM.

Supplementary Material

Refer to Web version on PubMed Central for supplementary material.

Acknowledgements:

This work was supported by NCI/NIH R01 CA256193 to KSMS, JDL and JWH.

References

1. Landreville S, Agapova OA, Harbour JW. Emerging insights into the molecular pathogenesis of uveal melanoma. Future Oncol. 2008;4(5):629–36. [PubMed: 18922120]
2. Schank TE, Hassel JC. Immunotherapies for the Treatment of Uveal Melanoma-History and Future. Cancers (Basel). 2019;11(8).
3. Onken MD, Worley LA, Tuscan MD, Harbour JW. An accurate, clinically feasible multi-gene expression assay for predicting metastasis in uveal melanoma. J Mol Diagn. 2010;12(4):461–8. [PubMed: 20413675]
4. Field MG, Harbour JW. Recent developments in prognostic and predictive testing in uveal melanoma. Curr Opin Ophthalmol. 2014;25(3):234–9. [PubMed: 24713608]
5. Van Raamsdonk CD, Bezrookove V, Green G, Bauer J, Gaugler L, O'Brien JM, et al. Frequent somatic mutations of GNAQ in uveal melanoma and blue naevi. Nature. 2009;457(7229):599–602. [PubMed: 19078957]
6. Van Raamsdonk CD, Griewank KG, Crosby MB, Garrido MC, Vemula S, Wiesner T, et al. Mutations in GNA11 in uveal melanoma. N Engl J Med. 2010;363(23):2191–9. [PubMed: 21083380]
7. Vader MJC, Madigan MC, Versluis M, Suleiman HM, Gezgin G, Gruis NA, et al. GNAQ and GNA11 mutations and downstream YAP activation in choroidal nevi. Br J Cancer. 2017;117(6):884–7. [PubMed: 28809862]
8. Musi E, Ambrosini G, de Stanchina E, Schwartz GK. The phosphoinositide 3-kinase alpha selective inhibitor BYL719 enhances the effect of the protein kinase C inhibitor AEB071 in GNAQ/GNA11-mutant uveal melanoma cells. Mol Cancer Ther. 2014;13(5):1044–53. [PubMed: 24563540]
9. Yu FX, Luo J, Mo JS, Liu G, Kim YC, Meng Z, et al. Mutant Gq/11 promote uveal melanoma tumorigenesis by activating YAP. Cancer Cell. 2014;25(6):822–30. [PubMed: 24882516]
10. Yoo JH, Shi DS, Grossmann AH, Sorensen LK, Tong Z, Mleynek TM, et al. ARF6 Is an Actionable Node that Orchestrates Oncogenic GNAQ Signaling in Uveal Melanoma. Cancer Cell. 2016;29(6):889–904. [PubMed: 27265506]
11. Vaque JP, Dorsam RT, Feng X, Iglesias-Bartolome R, Forsthoefel DJ, Chen Q, et al. A genome-wide RNAi screen reveals a Trio-regulated Rho GTPase circuitry transducing mitogenic signals initiated by G protein-coupled receptors. Mol Cell. 2013;49(1):94–108. [PubMed: 23177739]
12. Feng X, Degese MS, Iglesias-Bartolome R, Vaque JP, Molinolo AA, Rodrigues M, et al. Hippo-independent activation of YAP by the GNAQ uveal melanoma oncogene through a trio-regulated rho GTPase signaling circuitry. Cancer Cell. 2014;25(6):831–45. [PubMed: 24882515]
13. Carvajal RD, Sosman JA, Quevedo JF, Milhem MM, Joshua AM, Kudchadkar RR, et al. Effect of selumetinib vs chemotherapy on progression-free survival in uveal melanoma: a randomized clinical trial. Jama. 2014;311(23):2397–405. [PubMed: 24938562]
14. Carvajal RD, Piperno-Neumann S, Kapiteijn E, Chapman PB, Frank S, Joshua AM, et al. Selumetinib in Combination With Dacarbazine in Patients With Metastatic Uveal Melanoma: A Phase III, Multicenter, Randomized Trial (SUMIT). Journal of Clinical Oncology. 2018;36(12):1232–9. [PubMed: 29528792]
15. Faiao-Flores F, Emmons MF, Durante MA, Kinose F, Saha B, Fang B, et al. HDAC Inhibition Enhances the In Vivo Efficacy of MEK Inhibitor Therapy in Uveal Melanoma. Clin Cancer Res. 2019;25(18):5686–701. [PubMed: 31227503]
16. Butler A, Hoffman P, Smibert P, Papalexi E, Satija R. Integrating single-cell transcriptomic data across different conditions, technologies, and species. Nat Biotechnol. 2018;36(5):411–20. [PubMed: 29608179]
17. Emmons MF, Faiao-Flores F, Sharma R, Thapa R, Messina JL, Becker JC, et al. HDAC8 Regulates a Stress Response Pathway in Melanoma to Mediate Escape from BRAF Inhibitor Therapy. Cancer Res. 2019;79(11):2947–61. [PubMed: 30987999]
18. Landreville S, Agapova OA, Matatall KA, Kneass ZT, Onken MD, Lee RS, et al. Histone deacetylase inhibitors induce growth arrest and differentiation in uveal melanoma. Clin Cancer Res. 2012;18(2):408–16. [PubMed: 22038994]

19. Flaherty KT, Robert C, Hersey P, Nathan P, Garbe C, Milhem M, et al. Improved survival with MEK inhibition in BRAF-mutated melanoma. The New England journal of medicine. 2012;367(2):107–14. [PubMed: 22663011]
20. Durante MA, Rodriguez DA, Kurtenbach S, Kuznetsov JN, Sanchez MI, Decatur CL, et al. Single-cell analysis reveals new evolutionary complexity in uveal melanoma. Nat Commun. 2020;11(1):496. [PubMed: 31980621]
21. Stuart T, Butler A, Hoffman P, Hafemeister C, Papalexi E, Mauck WM 3rd, et al. Comprehensive Integration of Single-Cell Data. Cell. 2019;177(7):1888–902 e21. [PubMed: 31178118]
22. Gundersen GW, Jones MR, Rouillard AD, Kou Y, Monteiro CD, Feldmann AS, et al. GEO2Enrichr: browser extension and server app to extract gene sets from GEO and analyze them for biological functions. Bioinformatics. 2015;31(18):3060–2. [PubMed: 25971742]
23. Faiao-Flores F, Alves-Fernandes D, Pennacchi PC, Sandri S, Vicente ALSA, Scapulatempo-Neto C, et al. Targeting the hedgehog transcription factors GLI1 and GLI2 restores sensitivity to vemurafenib-resistant human melanoma cells. Oncogene. 2017;36(13):1849. [PubMed: 27748762]
24. Paraiso KH, Haarberg HE, Wood E, Rebecca VW, Chen YA, Xiang Y, et al. The HSP90 inhibitor XL888 overcomes BRAF inhibitor resistance mediated through diverse mechanisms. Clinical cancer research. 2012.
25. Faiao-Flores F, Suarez JA, Soto-Cerrato V, Espona-Fiedler M, Perez-Tomas R, Maria DA. Bcl-2 family proteins and cytoskeleton changes involved in DM-1 cytotoxic effect on melanoma cells. Tumour Biol. 2013;34(2):1235–43. [PubMed: 23341182]
26. Bi L, Ren Y, Feng M, Meng P, Wang Q, Chen W, et al. HDAC11 Regulates Glycolysis through the LKB1/AMPK Signaling Pathway to Maintain Hepatocellular Carcinoma Stemness. Cancer Res. 2021;81(8):2015–28. [PubMed: 33602787]
27. Smalley KSM. A pivotal role for ERK in the oncogenic behaviour of malignant melanoma? International Journal of Cancer. 2003;104(5):527–32. [PubMed: 12594806]
28. Carvajal RD, Piperno-Neumann S, Kapiteijn E, Chapman PB, Frank S, Joshua AM, et al. Selumetinib in Combination With Dacarbazine in Patients With Metastatic Uveal Melanoma: A Phase III, Multicenter, Randomized Trial (SUMIT). J Clin Oncol. 2018;36(12):1232–9. [PubMed: 29528792]
29. Maertens O, Kuzmickas R, Manchester HE, Emerson CE, Gavin AG, Guild CJ, et al. MAPK Pathway Suppression Unmasks Latent DNA Repair Defects and Confers a Chemical Synthetic Vulnerability in BRAF-, NRAS-, and NF1-Mutant Melanomas. Cancer Discov. 2019;9(4):526–45. [PubMed: 30709805]
30. Levinzon L, Madigan M, Nguyen V, Hasic E, Conway M, Cherepanoff S. Tumour Expression of Histone Deacetylases in Uveal Melanoma. Ocul Oncol Pathol. 2019;5(3):153–61. [PubMed: 31049320]
31. Gao L, Cueto MA, Asselbergs F, Atadja P. Cloning and functional characterization of HDAC11, a novel member of the human histone deacetylase family. J Biol Chem. 2002;277(28):25748–55. [PubMed: 11948178]
32. Liu SS, Wu F, Jin YM, Chang WQ, Xu TM. HDAC11: a rising star in epigenetics. Biomed Pharmacother. 2020;131:110607. [PubMed: 32841898]
33. Villagra A, Cheng F, Wang HW, Suarez I, Glozak M, Maurin M, et al. The histone deacetylase HDAC11 regulates the expression of interleukin 10 and immune tolerance. Nat Immunol. 2009;10(1):92–100. [PubMed: 19011628]
34. Thole TM, Lodrini M, Fabian J, Wuenschel J, Pfeil S, Hielscher T, et al. Neuroblastoma cells depend on HDAC11 for mitotic cell cycle progression and survival. Cell Death Dis. 2017;8(3):e2635. [PubMed: 28252645]
35. Gong D, Zeng Z, Yi F, Wu J. Inhibition of histone deacetylase 11 promotes human liver cancer cell apoptosis. Am J Transl Res. 2019;11(2):983–90. [PubMed: 30899397]
36. Sun L, Marin de Evsikova C, Bian K, Achille A, Telles E, Pei H, et al. Programming and Regulation of Metabolic Homeostasis by HDAC11. EBioMedicine. 2018;33:157–68. [PubMed: 29958910]

37. DeRan M, Yang J, Shen CH, Peters EC, Fitamant J, Chan P, et al. Energy stress regulates hippo-YAP signaling involving AMPK-mediated regulation of angiomotin-like 1 protein. Cell Rep. 2014;9(2):495–503. [PubMed: 25373897]

38. Wang W, Xiao ZD, Li X, Aziz KE, Gan B, Johnson RL, et al. AMPK modulates Hippo pathway activity to regulate energy homeostasis. Nat Cell Biol. 2015;17(4):490–9. [PubMed: 25751139]

39. Santinon G, Pocaterra A, Dupont S. Control of YAP/TAZ Activity by Metabolic and Nutrient-Sensing Pathways. Trends Cell Biol. 2016;26(4):289–99. [PubMed: 26750334]

40. Chua V, Han A, Bechtel N, Purwin TJ, Hunter E, Liao C, et al. The AMP-dependent kinase pathway is upregulated in BAP1 mutant uveal melanoma. Pigment Cell Melanoma Res. 2021.

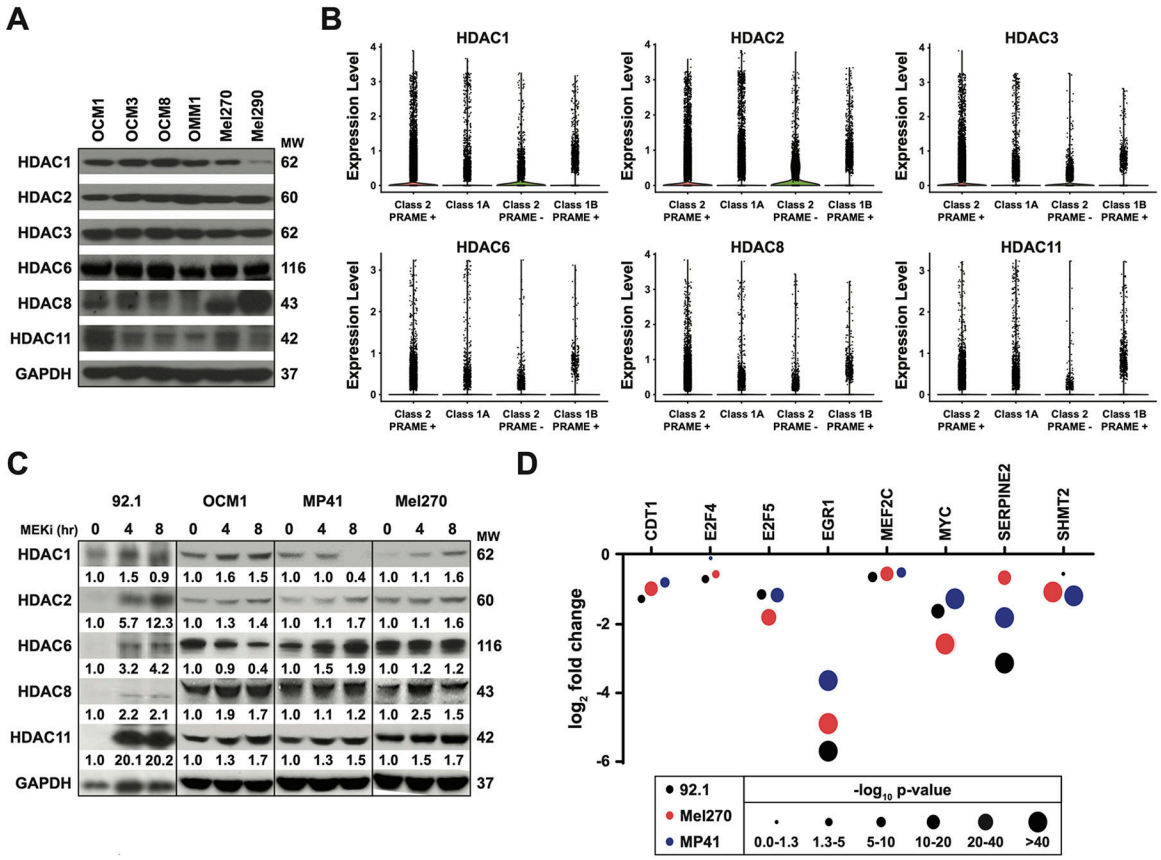

Figure 1: Treatment with a MEK inhibitor increases HDAC11 expression.

A)Multiple HDACs are expressed across UM cell lines. The UM cell lines OCM1, OCM3, OCM8, OMM1, Mel270 and Mel 290 were probed for HDAC1, HDAC2, HDAC3, HDAC6, HDAC8, HDAC11, and GAPDH by Western Blot. **B)** HDAC1, HDAC2, HDAC3, HDAC6, HDAC8, and HDAC11 expression levels are consistent across different classes of uveal melanoma in patients. Single cell RNA-Seq was analyzed from a cohort of uveal patients containing tumors from Class 1A, Class 1B PRAME+, Class 2 PRAME+ and Class 2 PRAME−. Shown are the gene expression levels of various HDACs. **C)** Treatment with a MEK inhibitor increases HDAC11 levels and decreases histone acetylation in UM. 92.1, OCM1, MP41 and Mel270 cells were treated a MEKi (trametinib, 10 nM) for 4 or 8 hours. Cells were subsequently probed for HDAC1, HDAC2, HDAC6, HDAC8, HDAC11 and GAPDH by western blot and quantified using ImageJ. **D)** HDAC11 target genes were significantly transcriptionally repressed after treatment with a MEK inhibitor. UM cells were treated with trametinib (10 nM) for 72 hours and RNA-Seq was performed. Genes identified to be transcriptionally repressed by HDAC11, including CDT1, E2F4, E2F5, EGR1, MEFC, MYC, SERPINE2, and SHMT2, were compared between MEKi and vehicle control populations.

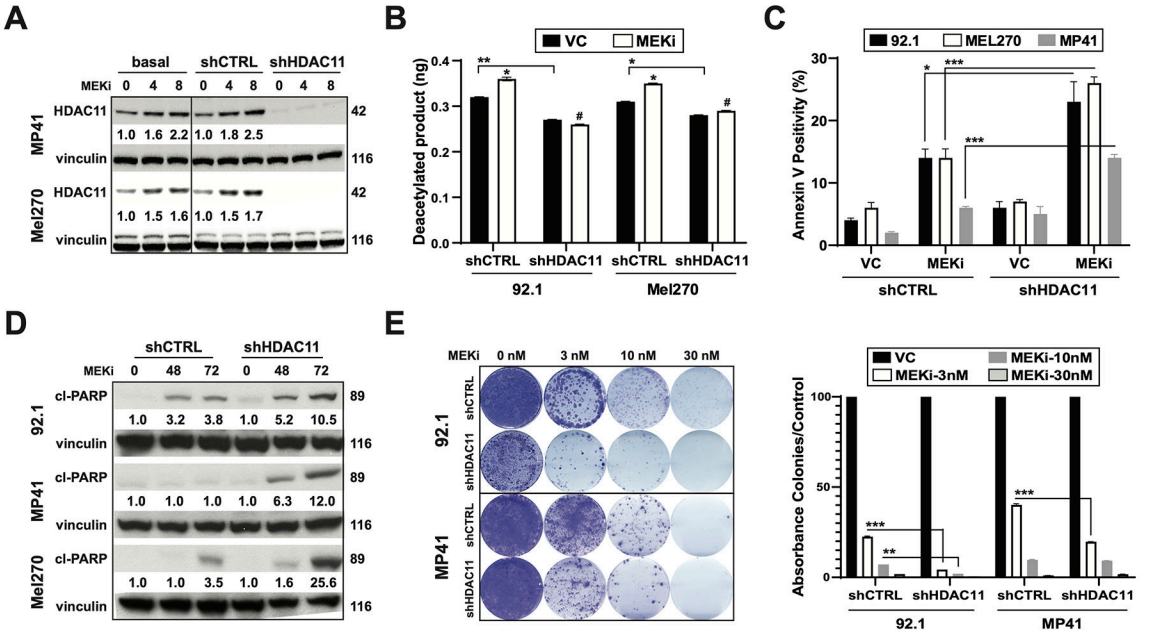

Figure 2: Silencing of HDAC11 increases sensitivity to MEK inhibition.

A) HDAC11 is knocked down in UM cell lines. shHDAC11, shCTRL, and basal uveal melanoma cell lines were treated with a MEKi (trametinib, 10 nM) for 4 or 8 hours. After treatment, the samples were probed for HDAC11 and vinculin expression by Western Blot Protein and quantified using ImageJ.. **B)** Silencing of HDAC11 reduced protein deacetylation. 92.1 and Mel270 cells transfected with shCTRL or shHDAC11 were treated with trametinib (10nM) for 48 hours and assayed for total protein acetylation. **C)** Silencing of HDAC11 increases MEKi-induced apoptosis in UM. shHDAC11 and shCTRL containing UM cell lines were treated with trametinib (30 nM) for 72 hours. Apoptosis was measured using Annexin V/PI staining by flow cytometry. **D)** Silencing HDAC11 induces apoptosis by caspase induced PARP cleavage. shHDAC11 and shCTRL containing UM cell lines were treated with trametinib (30 nM) for 48 or 72 hours. Samples were subsequently probed for cleaved PARP (cl-PARP) and vinculin expression followed by quantification with ImageJ. **E)** Silencing of HDAC11 increases long term sensitivity upon cell death in UM. shCTRL and shHDAC11 containing uveal melanoma cell lines were treated with trametinib (3 nM, 10 nM, or 30 nM) for 28 days. Colonies were stained with crystal violet and absorbance was read at 590 nm. Significances in **B)**, **C)** and **E)** were determined using one-way ANOVA followed by post-hoc t-test with * = $p<0.05$, ** = $p<0.01$, *** = $p<0.005$, and # = $p>0.05$. Experiments were repeated 3 times independently in triplicate.

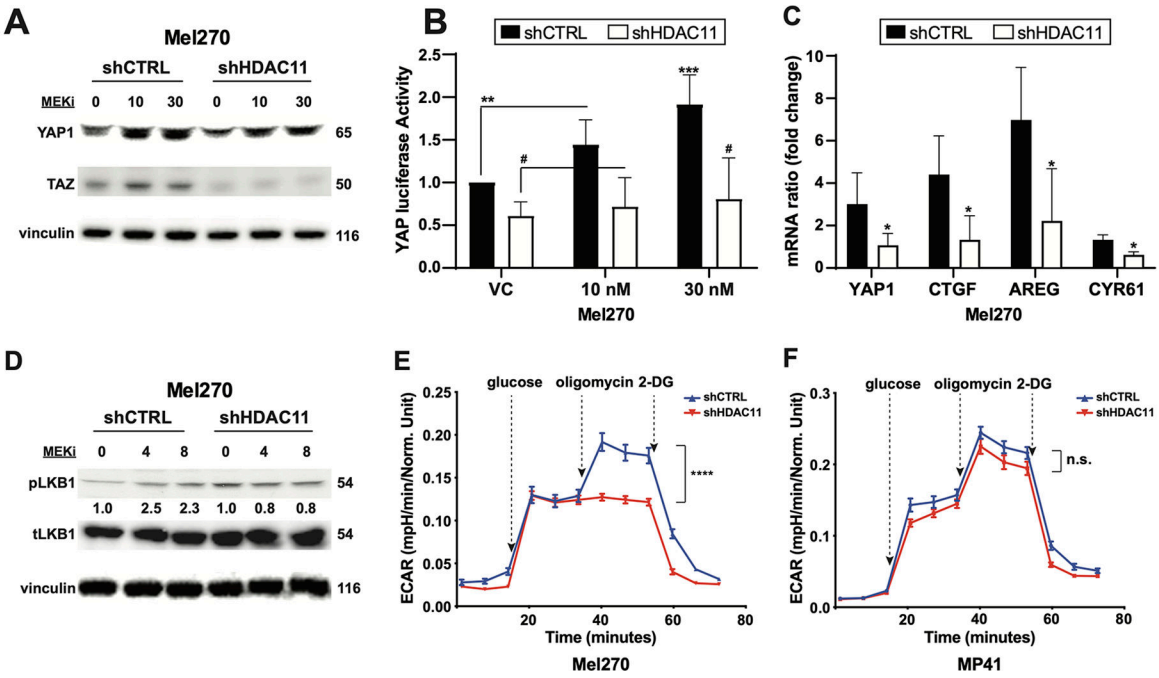

Figure 3: HDAC11 drives MEK inhibitor resistance in UM through upregulation of YAP/TAZ signaling.

A) Silencing of HDAC11 leads to decreased TAZ expression. shCTRL and shHDAC11 containing Mel270 cells were treated with a MEKi (trametinib, 10 nM or 30 nM) for 48 hours. Cells were probed for YAP1, TAZ, and vinculin expression by Western Blot. **B)** Silencing of HDAC11 decreases YAP/TAZ activity. shCTRL and shHDAC11 containing Mel270 cells were treated with trametinib (10 nM or 30 nM) for 48 hours. YAP/TAZ responsive 8xGTIIC-promoter activity was measured by luciferase assay. **C)** YAP/TAZ targeted gene expression was decreased upon HDAC11 inhibition. shCTRL and shHDAC11 containing Mel270 cells were treated with trametinib (10 nM) for 48 hours. qRT-PCR was performed on the YAP/TAZ targeted genes including YAP1, CTGF, AREG and CRY61 and normalized against 0h treatment. In **B-C)**, significance was determined using a one-way ANOVA followed by a post-hoc t-test with * = $p<0.05$, ** = $p<0.01$, ** = $p<0.005$, and # = $p>0.05$. **D)** Silencing of HDAC11 activates LKB1. shCTRL and shHDAC11 containing Mel270 cells were treated with trametinib (30 nM) for 0, 4 and 8 hours. Cells were probed for pLKB1, LKB1, and vinculin expression by Western Blot followed by quantification with ImageJ. **E-F)** Silencing of HDAC11 can decrease the rates of glycolysis under glycolytic stress in uveal melanoma. Seahorse XF glycolysis stress test assay on MEL270 **E)** and MP41 **F)**. Figure shows one representative experiment out of two independent experiments (2 biological replicates), visualizing 12 technical replicates within the experiment. Error bars represent Standard Error of the Mean. Student's t-test was performed on each of the 3 readings after oligomycin injection, representing the glycolytic reserve of each cell line. **** = $P<0.0001$.

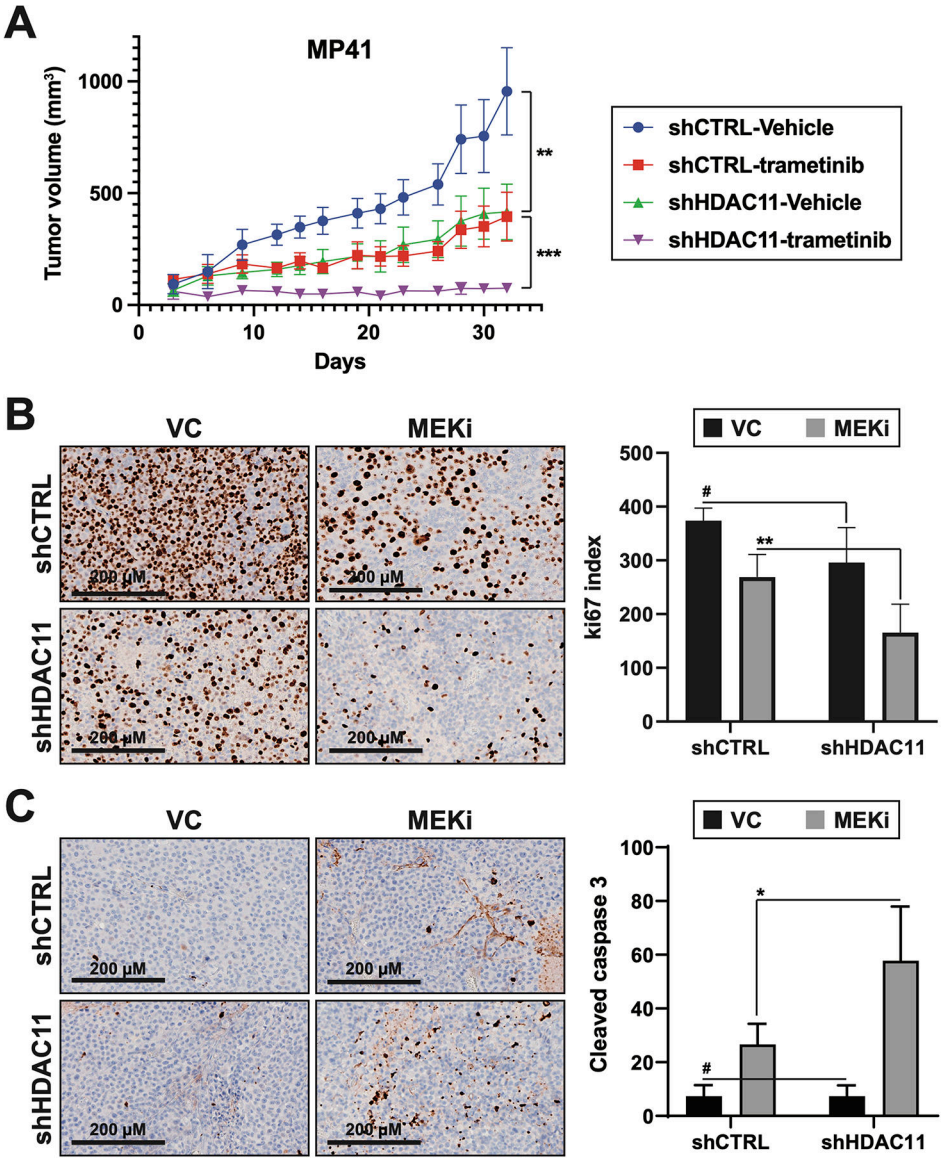

Figure 4: Silencing of HDAC11 limits escape from MEKi therapy in uveal melanoma mouse models.

A) shCTRL or shHDAC11 containing MP41 uveal melanoma cells (n=10 per treatment group) were xenografted into CB17-Prdkc scid/j mice and tumors allowed to form before being treated with MEKi (trametinib, 1 mg/kg oral gavage, daily) or VC for 32 days. Data show mean tumor volume +/− S.E. mean. **B)** Silencing HDAC11 decreases Ki67 expression after trametinib treatment. Samples from **A)** were stained with Ki67 by IHC. Positively stained cells for each treatment group were quantified (5 fields quantified per IHC sample). **C)** Silencing HDAC11 increases cleaved caspase3 staining. Samples from **A)** were stained with cleaved caspase 3 by IHC. Positively stained cells for each treatment group were quantified (5 fields quantified per IHC sample). In **A-C)**, significance was determined using a student's t-test with * = $p<0.05$, ** = $p<0.01$, *** = $p<0.005$, and # = $p>0.05$.